Defect and Diffusion Forum *Online: 2016-04-28*
ISSN: 1662-9507, Vol. 367, pp 140-148
doi:10.4028/www.scientific.net/DDF.367.140

Atomic Transport in Nano-crystalline Thin Films

Alain Portavoce[1, a], Khalid Hoummada[2,b] and Lee Chow[3,c]

[1]CNRS, IM2NP, Faculté des Sciences de Saint-Jérôme case 142, 13397 Marseille, France

[2]Aix-Marseille Université, IM2NP, Faculté des Sciences de Saint-Jérôme case 142, 13397 Marseille, France

[3]Department of Physics, University of Central Florida, Orlando, FL 32816, USA

[a]alain.portavoce@im2np.fr, [b]khalid.hoummada@im2np.fr, [c]Lee.Chow@ucf.edu

Keywords: Diffusion, Thin films, Nano-crystalline.

Abstract. Ge and B diffusion was studied in nano-crystalline Si, and Pd and Si self-diffusion was studied in nano-crystalline Pd_2Si during and after Pd/Si reactive diffusion. These experiments showed that grain boundary (GB) diffusion kinetic is the same in micro- and nano-GBs, whereas triple junction (TJ) diffusion is several orders of magnitude faster than GB diffusion. In addition, GB segregation and GB migration can significantly modify atomic diffusion profiles in nano-crystalline materials, and atomic transport kinetics can be largely increased in nano-grains compared to micro-grains, as well as during reactive diffusion, probably due to an increase of point defect concentration. These observations show that atomic transport in nanometric layers during reactive diffusion is complex, since GBs and TJs are moving and the proportion of GBs and TJs is changing during the layer growth.

Introduction

Thin film reactive diffusion is a process commonly used to produce embedded layers or multilayers as well as surface thin films exhibiting physical properties needed for different applications, such as correct interfacial work function and resistivity for electrical contact fabrication on transistor active zones in microelectronics [1-2]. With the development of nanotechnologies, the thickness of thin films has already reached the nanometric (nano-) scale [3-4]. In particular in microelectronics, the thickness of silicide layers located between the first metallic contact and doped-silicon, produced by the self-aligned silicide (SALICIDE) process [5-6], is usually lower than 50 nm [7]. In this case, the layer grown by reactive diffusion between a metallic film and the semiconductor has a nanometric thickness (nano-layer) and is nano-crystalline (nc) with nano-grains exhibiting an average size close to the thickness of the nano-layer [8]. Usually, thin film reaction is modeled considering atomic transport in the growing phase and atomic reaction at the growing phase interfaces [9-11]. Thus, in order to simulate reactive diffusion processes at the atomic scale, for process engineering for example, it is necessary to study the effect of the nano-sizes on atomic transport and reaction. In this paper, experimental results aiming to study the influence of nano-sizes [12-14] and of interfacial reaction [8] upon atomic transport during reactive diffusion are presented. In the first part, ideal atomic diffusion is studied in nc-Si layers without grain boundary (GB) migration and without reaction [12-13]. In the second part, atomic diffusion is studied in nc-Si layers experiencing GB migration as well as GB segregation [14]. Finally, in the third part, atomic self-diffusion is studied during interfacial reaction and without interfacial reaction in same silicide nc-layers [8]. All these experiments allow an interesting picture of atomic transport during the growth of nano-layers via reactive diffusion to be drawn.

Diffusion in nanocrystalline layers

Before considering atomic transport in growing nano-crystalline layers, a first step consists of studying atomic transport in nano-crystalline films. For example, Ge and Si are entirely miscible elements forming an ideal solid solution (no compound formation). In addition, Ge and Si films can

be produced with a very high purity (contaminations lower than 10^{15} at cm^{-3}), and Ge segregation was not observed in Si GBs. Thus, the study of Ge diffusion in nc-Si allows fundamental investigations on atomic transport in nanostructures to be performed. Indeed, nc-Si layers are made of nano-crystals (the nano-grains) and nano-interfaces (the nano-GBs), and contain a non-negligible amount of triple junctions (TJs) that result from GB intersections.

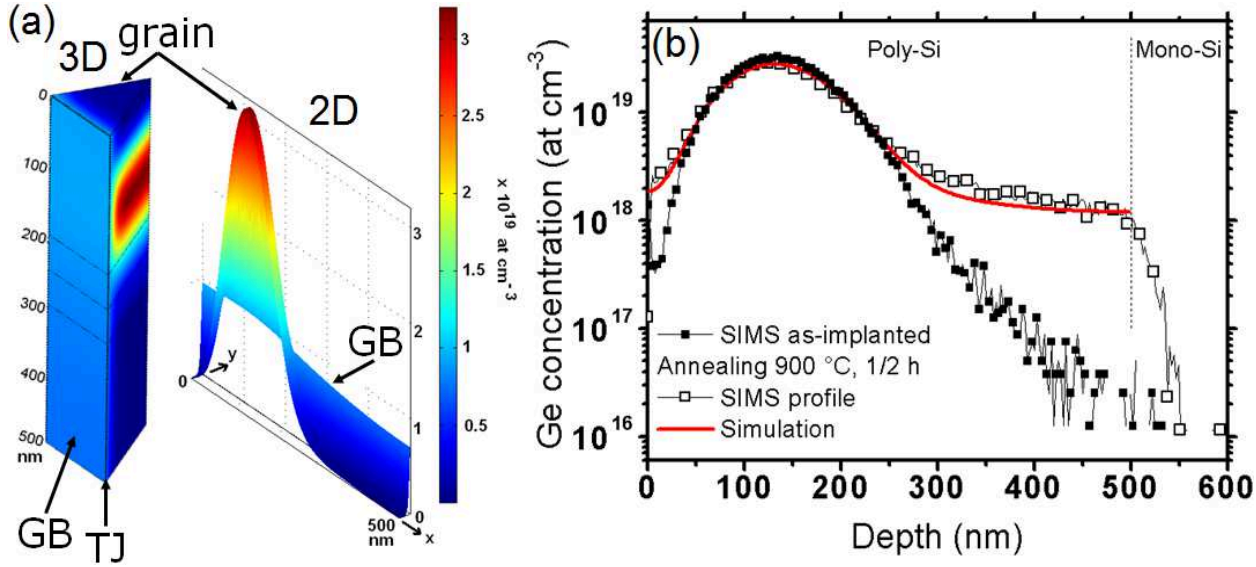

Figure 1. (a) 2D (grains and GBs diffusion paths) and 3D (grains, GBs, and TJs diffusion paths) geometries used for fitting experimental diffusion profiles by finite elements simulations, and (b) example of experimental SIMS profiles (symbols) fitted using 2D finite element simulations (red solid line).

In order to study Ge atomic transport in nc-Si, a 500 nm-thick nc-Si layer was deposited by chemical vapor deposition (CVD) at low temperature on an cleaned Si(001) substrate. The averaged grain size in the nc-Si was measured by X-ray diffraction and found to be 40 nm. Thus, a Ge dose of 4.2×10^{14} at cm^{-2} was implanted at room temperature in the nc-Si layer with an ion beam energy of 180 keV. After implantation, pieces of the sample were annealed under argon flow at different temperatures and for different times. The Ge diffusion profiles were measured by secondary ion mass spectrometry (SIMS). Grain growth was not observed during the sample annealing. Ge diffusivity was measured from the SIMS profiles using finite element simulations (FES) [12]. Two different models were used to fit the experimental Ge diffusion profiles: in the first one, only lattice diffusion in grains (D_g) and GB diffusion (D_{gb}) were taking into account using a usual two-dimensional (2D) geometry (Fig. 1a) [12]; whereas in the second one, Ge diffusion in grains, GBs as well as in TJs (D_{tj}) was taking into account using a three-dimensional (3D) geometry (Fig. 1a) [13]. The SIMS profiles could be fitted correctly with the two models, using the experimental as-implanted Ge SIMS profile as initial distribution (Fig. 1b) in the 2D or 3D geometries. With the 2D geometry, Ge diffusion in Si nano-grains was found to be one order of magnitude faster than in the Si monocrystal (mono-Si), with an activation energy ~ 1 eV lower than in mono-Si. Ge diffusion was also found to be faster in nano-GBs compared to micrometric (mico-) GBs. However, the diffusion activation energy was found to be almost the same in nano-GBs and micro-GBs. The same *Dg* as with the 2D geometry was found with the 3D geometry. However, the same GB diffusion coefficient as in micro-GBs was found in nano-GBs with the 3D geometry, and the Ge TJ diffusion coefficient was found to be ~ 3 orders of magnitude faster than in regular micro-GBs.

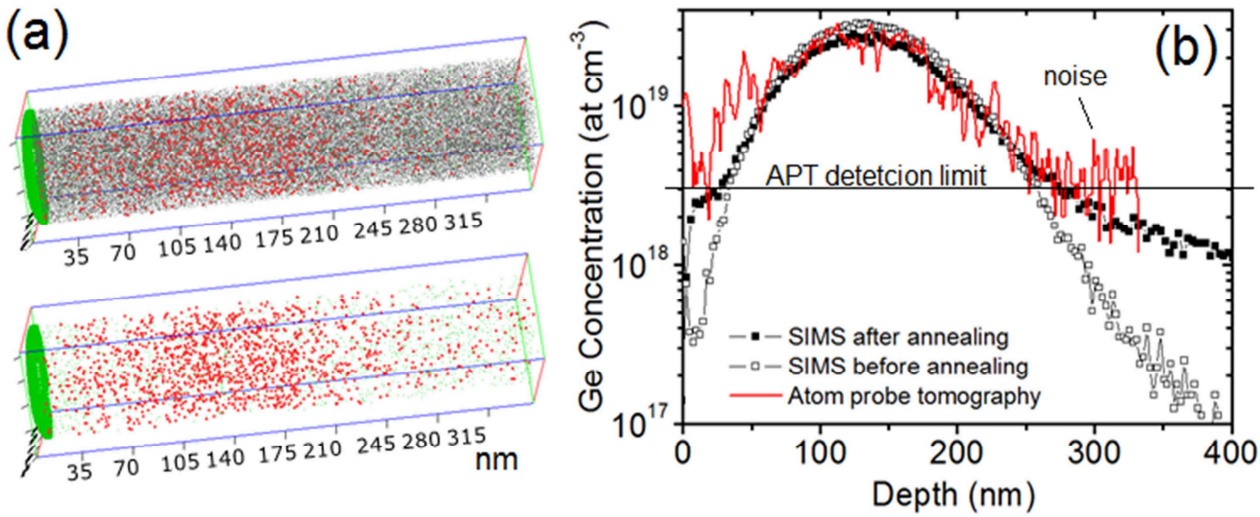

Fig. 2. APT analysis performed on an nc-Si layer implanted with Ge and annealed at 850 °C for one hour: (a) 3D distributions of Si (gray dots) and Ge (red dots) atoms, the green dots correspond to Ni atoms from a Ni cap deposited after annealing for APT sample preparation; (b) comparison between the SIMS profile (solid squares) and the APT profile (red solid line) measured in the volume presented in (a).

In order to check that the lattice diffusion found in nano-grains was actually faster than in nicro-grains, atom probe tomography (APT) was used to measure the Ge diffusion profile in nano-grains. Fig. 2 presents an APT analysis obtained in a volume of the sample annealed at 850 °C for one hour, exhibiting a lateral size close to the size of the nano-grains. Ge atoms are randomly distributed (Fig. 2a), no extended defects such as dislocations are detected [15-18], and the Ge diffusion profile measured in this volume is in good agreement with the SIMS profile measured in the same sample (Fig. 2b). Furthermore, no significant Ge concentration variations were noted in the direction perpendicular to the sample depth, which could be attributed to GB migration-mediated Ge redistribution. Thus, Ge atoms actually diffused in the nano-grains with the lattice diffusion coefficient deduced from the 2D and 3D FES, without the use of extended defects, and without notable influence of GB migration. The study of Ge diffusion in nc-Si shown that TJ diffusion is not negligible in nc-layers with 40 nm-wide grains. In addition, atomic transport in nanocrystals can be different from that in large monocrystals, probably due to a modification of point defect concentrations related to the size reduction. However, the GB nature, and thus, the concentration of point defects in GBs, do not change with the size reduction. This study also confirmed that TJs are linear defects exhibiting different properties than GBs, with different point defect concentrations and/or different diffusion mechanisms than in GBs, promoting faster atomic transport kinetic than in GBs. The results of this study are summarized in Fig. 3, comparing Ge diffusion coefficients in the different diffusion paths: lattice, nano-lattice, GBs, TJs, and surface. It is interesting to note that the TJ diffusion coefficient converges with the surface diffusion coefficient, and that the nano-lattice diffusion coefficient (in nano-crystals) converges with the regular lattice diffusion coefficient close to the Si melting temperature (T_m).

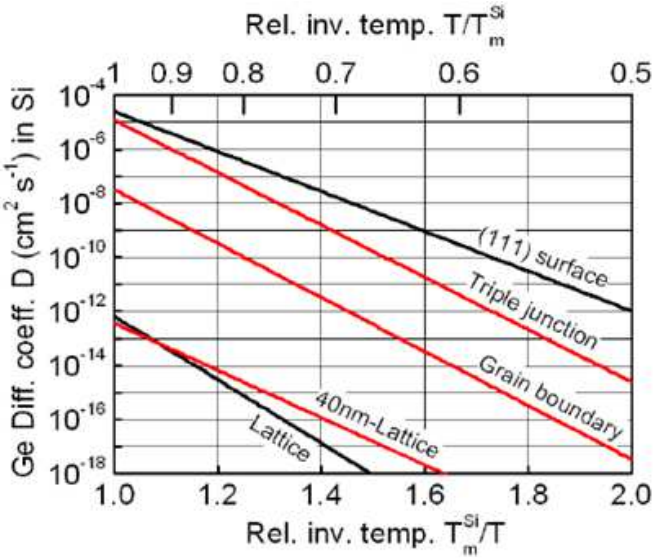

Figure 3. Comparison between the Ge diffusion coefficients measured in different diffusion paths in Si: monocrystalline Si, 40 nm-wide nano-grains, GBs, TJs, and (111) surface.

Grain boundary migration and segregation effects on diffusion in nanocrystalline layers

After studying atomic transport in nc-layers in the case of an ideal system such as Si and Ge, it is interesting to investigate more complex cases, such as B diffusion in nc-Si. Indeed, B is a *p*-type dopant in Si [19], thus, its lattice diffusion coefficient can vary with B concentration. In addition, B is known to segregate in Si GBs [20], which can influence GB migration [21-22]. In order to investigate B diffusion in nc-Si, a 250 nm-thick amorphous Si (a-Si) layer was deposited by low-pressure CVD at 530 °C on an oxidized Si(001) wafer exhibiting a surface oxide of ~ 12 nm. Thus, the sample was implanted with a B dose of 3.5×10^{14} at cm^{-2} with a beam energy of 7 keV. Pieces of the sample were annealed at different temperatures and for different times under vacuum (< 10^{-7} Torr). The B diffusion profiles were measured by SIMS [14]. The a-Si layer was shown to crystallize rapidly at temperatures higher than 550 °C, forming an nc-Si layer made of 50 nm-wide grains. During this process, a first B distribution was formed corresponding to the SIMS profile in fig. 4a measured after annealing at 550 °C for 24 hours. This B profile can be considered as the initial profile for diffusion in the nc-Si layer, since it mainly results from Si crystallization and not from B diffusion [14,23-24]. For example, after Si crystallization, the B profile does not change for low temperature (< 550 °C) and long-time (> 1 day) annealing. Fig. 4a shows that B atoms diffuse in the nc-Si layer at temperatures higher than 600 °C.

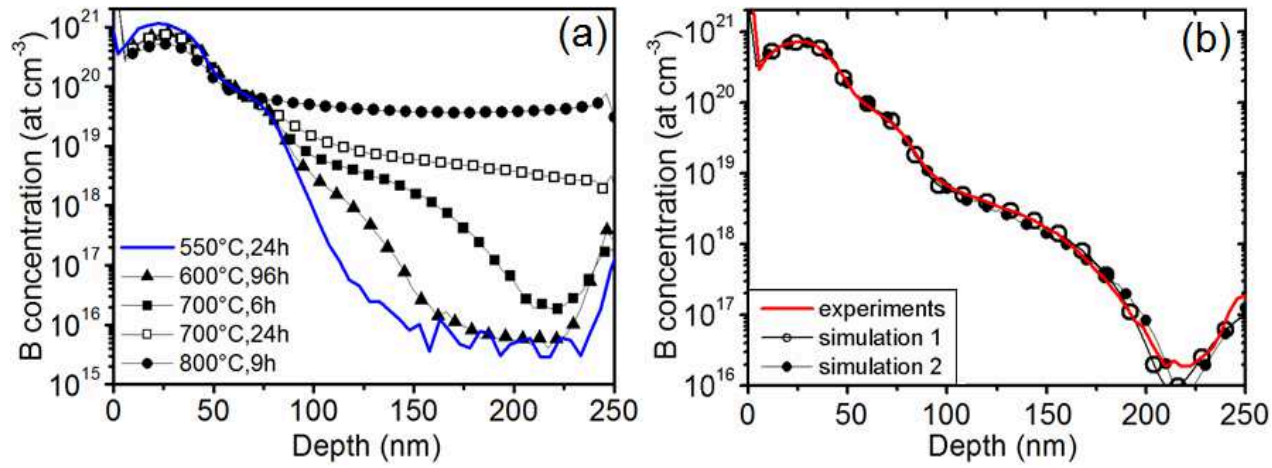

Figure 4. (a) Experimental B diffusion profiles measured by SIMS in nc-Si; and (b) comparison between the B SIMS profile measured in the sample annealed at 700 °C for 6 hours (red solid line) to B diffusion profiles simulated using two different expression of the GB migration rate: $v_{gb} = a - bt^{1/2}/C_B^*$ for simulation 1 (open circles) and $v_{gb} = k_0/2C_B^* t^{1/2}$ for simulation 2 (solid circles).

This Figure also shows that the B diffusion profile forms a shoulder before to reach a constant composition, once the B solubility limit in Si has been reached. This shoulder does not correspond to the usual diffusion profile observed in polycrystalline materials, which exhibit in general a linear slope at the end of the profile due to the diffusion in GBs [25]. 2D FES were used to fit the B experimental profiles using the well-known diffusion models of B diffusion in the Si lattice, taking into account the variation of the B diffusion coefficient versus B concentration related to the variation of the Si Fermi level with B concentration [14], as well as B diffusion in Si GBs [14]. The SIMS profiles measured in nc-Si (Fig. 4a) could not be reproduced by the usual B diffusion model, even if B GB segregation was taken into account [14,26]. The study of the grain size distribution by atomic force microscopy (AFM) showed that the average size of the nano-grains did not change after the different annealing. However, depending on the annealing conditions, several distributions of grain size was observed with a negligible density compared to the density corresponding to the average size. Thus, contrasting with the study of Ge diffusion in nc-Si described in the previous section, grain boundary migration occurred during annealing, even if the average size of the nano-grains could be considered to be constant [14,23-24]. Several reasons could explain that the grains have grown in the B-implanted samples (BIS) and not in the Ge-implanted samples (GIS): i) the Si nc-layer was directly produced during CVD for the GIS, maybe stabilizing the grains due to GB passivation by H, whereas the nc-Si layer was produced by a-Si crystallization during diffusion annealing in the case of the BIS; ii) the nc-Si layer was deposited on a monocrystalline Si(001) sample for the GIS, leading to a possible coherency between some nano-grains and the Si substrate at the nc-Si/mono-Si interface, whereas the a-Si layer crystallized on an amorphous SiO_2 film in the case of the BIS; and iii) the GIS samples were annealed under argon flux, whereas the BIS were annealed under vacuum. A 2D model describing B diffusion in nc-Si taking into account GB migration was determined. In this model, the B diffusion coefficients were set to be constant in nano-grains and GBs. D_{gb} was taken from the literature, and D_g was adjusted in order to obtain the best fit of the experimental profiles. GBs were moving with a migration rate v_{gb}, and B atoms were considered to be incorporated in the Si nano-grains after the lateral migration of the GBs. As shown in Fig. 4b, the experimental B diffusion profiles could be perfectly fitted by the model if the GB migration rate was set to be inversely proportional to the B concentration (C_B^*), either using a standard GB migration rate description $v_{gb} = k_0/2C_B^* t^{1/2}$ (solid circles in Fig. 4b) or $v_{gb} = a - bt^{1/2}/C_B^*$ (open circles in Fig. 4b). The decrease of GB migration rate with the increase of B concentration is in agreement with the pinning of Si GBs with B GB segregation [27]. We noted that the B lattice diffusion coefficient was found to be one order of magnitude slower than the expected B lattice diffusion coefficient taking into account electrical effects. B diffusion is mainly self-interstitial-mediated in Si, whereas Ge diffusion is mainly vacancy-mediated. As the self-interstitial concentration usually decreases when the vacancy concentration increases in Si, a decrease of B diffusion kinetic and an increase of Ge diffusion kinetic in Si nano-grains are in agreement with an increase of the vacancy concentration in Si nano-grains compared to that in mono-Si.

Interfacial reaction effect on diffusion during nano-crystalline layer growth

The previous observations showed that in nc-layer i) atomic transport can be faster in nano-grains for vacancy-mediated impurities, ii) atomic transport kinetic may be increased due to TJ diffusion, and iii) atomic diffusion can be modified due to atomic GB segregation and GB migration. In this section, the influence of interfacial reaction on atomic transport is investigated during silicide growth at low temperature. Indeed, during silicidation, a silicide nc-layer is formed between a thin metallic film and a Si substrate, and in addition to the GB migration effect on atomic transport due to the layer growth, the metal/Si reaction at the two interfaces metal/Si and Si/metal can influence atomic transport in the silicide during growth. In order to investigate self-diffusion with and without interfacial reaction, we studied the low-temperature growth of Pd_2Si by in situ ultrahigh vacuum (UHV) Auger electron spectroscopy (AES) [8]. Indeed, the low-T reaction of a Pd nano-film on Si leads to the formation of the single phase Pd_2Si, allowing the study to be simplified; and the in situ

study of the atomic surface concentration kinetic variations by AES during atom dissolution or segregation on a given substrate was shown to inform on atomic diffusion kinetic in the bulk of the considered substrate [28-31]. Thus, *in situ* UHV AES can allow the self-diffusion coefficients in a compound to be measured in the same sample during the reactive diffusion growth of the compound and after the growth of the compound. For each measurement a Si(001) substrate (~ 0.5 × 0.8 cm^2) was loaded in the AES UHV chamber. Thus the substrate surface was in situ cleaned by Ar^+ ion bombardment with a beam energy of 2 keV, and heated at 500 °C for a few minutes. After the cleaning step, a 30 nm-thick Pd layer was *in situ* deposited at room temperature on the substrate surface by molecular beam deposition (MBD) via thermal evaporation with a growth rate of ~1 nm per minute. Therefore, the Pd MNN(330 eV) and the Si LMM(92 eV) Auger transition signals were recorded in real time during sample isothermal annealing. Five different measurements at five different annealing temperatures (115, 135,155, 175, and 195 °C) were performed [8].

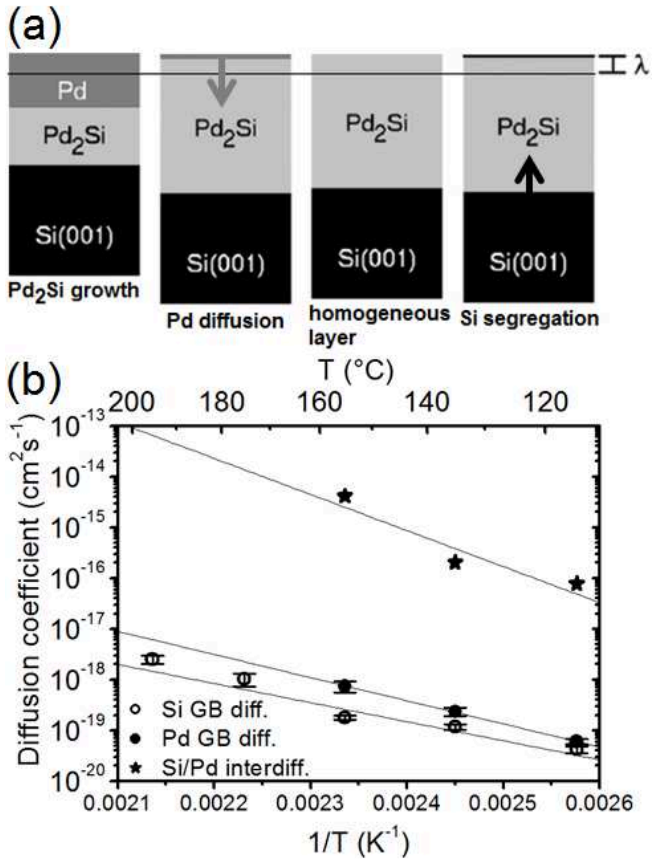

Figure 5. (a) Schematic summarizing the different steps occurring during Pd/Si reactive diffusion, λ corresponds to the depth probed by AES; and (b) comparison between the effective self-diffusion coefficient measured during Pd_2Si growth via Pd/Si reactive diffusion (solid stars) and the Si (open circles) and Pd (solid circles) self-diffusion coefficients measured in the same Pd_2Si layer after growth.

Fig. 5a presents schematically the different steps that took place during isothermal annealing [8]. In this schematic λ corresponds to the depth probed by AES (~ 3 to 4 atomic monolayers). In a first step, after Pd_2Si nucleation, Pd atoms diffused in the Pd_2Si layer to react at the Pd_2Si/Si interface and Si atoms diffused in Pd_2Si to react at the Pd_2Si/Pd interface allowing for the growth of the Pd_2Si layer by reactive diffusion. During this step, the surface composition stayed pure in Pd (the Si concentration C_{Si} ~ 0). When the Pd_2Si/Pd interface entered in the region probed by AES (first detection of the Si signal after a time Δt_{Si}), the reaction was almost finished, and only ~ 4 Pd monolayers (MLs) were still present on the Pd_2Si surface. In a second step, since Pd exhibits a higher surface energy than Si [8], these four Pd MLs were dissolved into the Pd_2Si bulk until reaching a concentration similar to that of the Pd_2Si phase (C_{Si} ~ 0.33). Thus, in order to minimize Pd_2Si surface energy, Si atoms segregated on the Pd_2Si surface (C_{Si} > 0.33). Considering the usual model of reactive diffusion corresponding to our experience conditions [8], the effective self-diffusion coefficient D_{eff} of Si and Pd atoms in Pd_2Si could be determined at three different temperatures (solid stars in Fig. 5b) thanks to the measurements of Δt_{Si}. This diffusion coefficient is found to be a little larger than that reported in the literature. However, one has to note that our

samples are purer than that of the literature since they were made by UHV MBD instead of by sputtering, which can explain an increase of atomic diffusivity in our samples [8]. The Pd dissolution kinetic and the Si surface segregation kinetic recorded by AES allowed the Pd (D_{Pd}, solid circles in Fig. 5b) and the Si (D_{Si}, open circles in Fig. 5b) self-diffusion coefficients to be measured in the same Pd_2Si layer after the growth. As shown in Fig. 5, the Pd and Si self-diffusion coefficients were found to be similar in Pd_2Si, as expected from the experiments reported in the literature using interfacial markers during Pd/Si reactive diffusion [32]. In addition, the Si self-diffusion coefficient measured by AES was found to be close to that measured by Egan and Comrie using SIMS profiles [33]. The three coefficients D_{eff}, D_{Pd}, and D_{Si} being measured in the same sample, in same experimental conditions, the comparison of these three coefficients bears a minimum error. However, one can note that D_{eff} is at least three orders of magnitude larger than D_{Pd} and D_{Si}. Consequently, atomic transport kinetic is significantly increased during interfacial reaction. The diffusion coefficient of an impurity being equal to the product of the point defect concentration and the point defect diffusion coefficient, the increase of Pd and Si self-diffusion in Pd_2Si during reaction may be explained by an increase of the concentration of point defects in the growing layer. In particular, interfacial Pd/Si reaction was shown to inject point defects in Si by diffusion due to an increase of point defect concentration at the Pd_2Si/Si interface [34-36]. Thus, one can also think that an increase of point defects at the Pd_2Si/Pd and Pd_2Si/Si interfaces may lead to point defect injection in the Pd_2Si layer, allowing a steady state to be reached between the point defect diffusion flux from the interfaces and the point defect annihilation kinetic at point defect sinks during reaction at low temperature, promoting faster Pd and Si self-diffusion.

Summary

The study of Ge and B diffusion in nc-Si, as well as the study Pd and Si self-diffusion in Pd_2Si during reactive diffusion allow several conclusions to be made concerning atomic transport in nc-layers: i) the faster atomic diffusivity observed in nc-materials is not due to faster diffusion in nano-GBs, but to fast diffusion in TJs and enhanced diffusion for vacancy mediated impurities in nano-grains, ii) impurity GB segregation can influence GB migration rate promoting a significant modification of the impurity diffusion profile, and iii) during thin film reactive diffusion, the atomic transport kinetic can be increased of several orders of magnitude, probably due to point defect injection from the interfaces were a reaction takes place. Thus, the atomic transport in nano-layers during their growth by reactive diffusion appears to be complex since i) the proportion of GBs and TJs changes versus time, meaning that the diffusion paths and the point defect sinks are modified when the thickness of the layer increases, ii) GB and TJ migration take place during the growth, and iii) the reactions located at the two interfaces of the growing layer being different, different point defects can be injected from these two interfaces, depending on the chemical reaction and on the stress state of the interfaces.

References

[1] S.M. Sze: *VLSI Technology* (International Edition, Singapore, 1988), p. 397.

[2] M.A. Nicolet and S.S. Lau: *VLSI Electronics, Microstructure Science*(Academic Press, New York, 1983), Vol. 6, p. 330

[3] C. Lavoie, F. M. d'Heurle, C. Detavernier, and C. Cabral, Jr.: Microelectron. Eng. Vol. 70 (2003), p. 144

[4] S. Bonnetier, B. Imbert, M. Hopstaken, D. Galpin, R. Gwoziecki, D. Barge, S. Zoll, O. Anilturk, E. Sicurani, C. Caillat, A. Barr, R. Gonella, Y. Espinoux, P. Mur, N. Mayet, A. Gotti, and M.-T. Basso: Microelectron. Eng. Vol. 84 (2007), p. 2528

[5] B.-Y. Tsaur and C. H. Anderson, Jr.: Appl. Phys. Lett. Vol. 47 (1985), p. 525

[6] P. Gas, C. Girardeaux, D. Mangelinck, and A. Portavoce: Mat. Sci. Eng. B Vol. 101 (2003), p. 43

[7] T. Schram, A. Spessot, R. Ritzenthaler, E. Rosseel, C. Caillat, and N. Horiguchi: Microelec. Eng. Vol. 120 (2014), p. 157

[8] A. Portavoce, K. Hoummada, F. Dahlem: Surf. Sci. Vol. 624 (2014), p. 135

[9] U. Gosele, K.N. Tu: J. Appl. Phys. Vol. 53 (1982), p. 3252

[10] F.M. d'Heurle and P. Gas: J. Mater. Res. Vol. 1 (1986), p. 205

[11] A. Portavoce and G. Tréglia: Phys. Rev. B Vol. 82 (2010), p. 205431

[12] A. Portavoce, G. Chai, L. Chow, and J. Bernardini: J. Appl. Phys. Vol. 104 (2008), p. 104910

[13] A. Portavoce, L. Chow, and J. Bernardini: Appl. Phys. Lett. Vol. 96 (2010), p. 214102

[14] A. Portavoce: Scripta Mater. Vol. 99 (2015), p. 37

[15] S. Duguay, T. Philippe, F. Cristiano, and D. Blavette: Appl. Phys. Lett. Vol. 97 (2010), p. 242104

[16] D. Mangelinck, K. Hoummada, A. Portavoce, C. Perrin, R. Daineche, M. Descoins, D.J. Larson and P.H. Clifton: Scripta Mater. Vol. 62 (2010), p. 568

[17] K. Hoummada, G. Tellouche, I. Blum, A. Portavoce, M. Descoins, and D. Mangelinck: Microelec. Eng. Vol. 107 (2013), p. 184

[18] A. Portavoce, O. Abbes, A. Spiesser, C. Girardeaux, L. Michez, and V. Le Thanh: Scripta Mater. Vol. 100 (2015), p. 70

[19] D. De Salvador, E. Napolitani, S. Mirabella, E. Bruno, G. Impellizzeri, G. Bisognin, E.F. Pecora, F. Priolo, and A. Carnera: Mat. Sci. Eng. B Vol. 154–155 (2008), p. 240

[20] S. Jin, K.S. Jones, M.E. Law, and R. Camillo-Castillo: J. Appl. Phys. Vol. 111 (2012), p. 044508

[21] J.W. Cahn: Acta Metal. Vol. 10 (1962), p. 789

[22] S.G. Kim and Y.B. Park: Acta Mater. Vol 56 (2008), p. 3739

[23] A. Portavoce, R. Simola, D. Mangelinck, J. Bernardini1, and P. Fornara: Diffusion and Defect Data Vol. 264 (2007), p. 33

[24] A. Portavoce, D. Mangelinck, R. Simola, R. Daineche, and J. Bernardini: Defect and Diffusion Forum Vols. 289-292 (2009), p. 329

[25] H. Mehrer: *Diffusion in Solids* (Springer-Verlag, Berlin Heidelberg, 2007).

[26] A. Portavoce, I. Blum, L. Chow, J. Bernardini, D. Mangelinck: Defect and Diffusion Forum Vols. 309-310 (2011), p. 63

[27] F. Liu, G. Yang, H. Wang, Z. Chen, and Y. Zhou: Thermochimica Acta vol. 443 (2006), p. 212

[28] A. Rolland and J. Bernardini: Scripta Metal. Vol. 19 (1985), p. 839

[29] A. Rolland, J. Bernardini, G. Moya, C. Girardeaux: Surf. Sci. Vol. 566–568 (2004), p. 1163

[30] Z. Balogh, Z. Erdélyi, D.L. Beke, G.A. Langer, A. Csik, H.-G. Boyen, U. Wiedwald, P. Ziemann, A. Portavoce, and C. Girardeaux: Appl. Phys. Lett. Vol. 92 (2008), p. 143104

[31] Z. Balogh, Z. Erdélyi, D.L. Beke, A. Portavoce, C. Girardeaux, J. Bernardini, and A. Rolland: Appl. Surf. Sci. 255 (2009), p. 4844

[32] E.C. Zingu, J.W. Mayer, C. Comrie, and R. Pretorius: Phys. Rev. B Vol. 30 (1984), p. 5916

[33] J.M. Egan and C.M. Comrie: Phys. Rev. B Vol. 40 (1989), p. 11670

[34] M. Seibt and K. Graff: J. Appl. Phys. Vol. 63 (1988), p. 4444

[35] M. Ronay and R.G. Schad: Phys. Rev. Lett. Vol. 64 (1990), p. 2042

[36] J.E. Masse, P. Knauth, P. Gas, and A. Charaï: J. Appl. Phys. Vol. 77 (1995), p. 934